APB *Advanced Pharmaceutical Bulletin*, **2012**, 2(1), 43-56
http://apb.tbzmed.ac.ir/

Design of vancomycin RS-100 nanoparticles in order to increase the intestinal permeability

Badir Delf Loveymi[1,2], Mitra Jelvehgari[1,3*], Parvin Zakeri-Milani[1,4], Hadi Valizadeh[1,5]

[1] *Faculty of Pharmacy, Tabriz University of Medical Sciences, Tabriz, Iran.*

[2] *Biotechnology Research Center, Tabriz University of Medical Sciences, Tabriz, Iran.*

[3] *Drug Applied Research Center, Tabriz University of Medical Sciences, Tabriz, Iran.*

[4] *Liver and Gastrointestinal Diseases Research Center, Tabriz University of Medical Sciences, Tabriz, Iran.*

[5] *Research Center for Pharmaceutical Nanotechnology, Tabriz University of Medical Sciences, Tabriz, Iran.*

ARTICLE INFO

Article Type:
Research Article

Article History:
Received: 10 Jan 2012
Accepted: 30 Jan 2012
ePublished: 15 Feb 2012

Keywords:
Vncomycin
Nanoparticles
Eudragit RS100
Physicochemical properties

ABSTRACT

***Purpose*:** The purpose of this work was to preparation of vancomycin (VCM) biodegradable nanoparticles to improve the intestinal permeability, using water-in-oil-in-water (W/O/W) multiple emulsion method. ***Methods*:** The vancomycin-loaded nanoparticles were created using double-emulsion solvent evaporation method. Using Eudragit RS100 as a coating material. The prepared nanoparticles were identifyed for their micromeritic and crystallographic properties, drug loading, particle size, drug release, Zeta potential, effective permeability (P_{eff}) and oral fractional absorption. Intestinal permeability of VCM nanoparticles was figured out, in different concentrations using SPIP technique in rats. ***Results*:** Particle sizes were between 362 and 499 nm for different compositions of VCM-RS-100 nanoparticles. Entrapment efficiency expansed between 63%-94.76%. The highest entrapment efficiency 94.76% was obtained when the ratio of drug to polymer was 1:3. The in vitro release studies were accomplished in pH 7.4. The results showed that physicochemical properties were impressed by drug to polymer ratio. The FT-IR, XRPD and DSC results ruled out any chemical interaction betweenthe drug and RS-100. Effective intestinal permeability values of VCM nanoparticles in concentrations of 200, 300 and 400 µg/ml were higher than that of solutions at the same concentrations. Oral fractional absorption was achieved between 0.419-0.767. ***Conclusion*:** Our findings suggest that RS-100 nanoparticles could provide a delivery system for VCM, with enhanced intestinal permeability.

Introduction

Vancomycin is a glycopeptide antibiotic that has been in clinical use for nearly 50 years to treat methicillin-resistant Staphylococcus aureus infections (1). It is water soluble, having a high molecular weight, and poorly absorbed after oral administration. It is well known that VCM, is very poorly absorbed from the GI tract, usually generating serum concentrations that are minimal or undetectable (2-5) . VCM was very stable in the supernatant of intestinal mucosal homogenate and that its binding to gastric mucin.VCM exhibited a secretory-oriented manner in both the jejunum and ileum. known P-glycoprotein modulators, significantly enhanced the serosal -to- mucosal permeation of VCM. It was suggested that intestinal P-glycoprotein might be involved in the poor absorption of VCM from rat small intestine as a potent barrier (6). Nanoparticulate polymeric delivery systems have been investigated as a possible accessibility to increase the oral drug availability. Biodegradable particulate carrier systems are of interest as potential means for oral delivery to enhance drug absorption, improve bioavailability and targeting of therapeutic agents to specific organ (7-10), because it is nontoxic biodegradable polymer and well tolerated by the human body. Eudragit RS-100 is a polymer has been commonly employed for the preparation of controlled-release oral pharmaceutical dosage forms (11). As Eudragit RS-100 is insoluble at physiological pH values, therefore it has been utilized as a good polymer for the preparation of pH-independent sustained-release formulations of drugs. Various non-biodegradable polymers with good biocompatibility such as Eudragit and ethyl cellulose were used in the preparation of nanospheres (11). The presence of a polymeric wall supplies a protection from

***Corresponding author:** Mitra Jelvehgari (PHD), Department of Pharmaceutics, Faculty of Pharmacy, Tabriz University of Medical Sciences, Tabriz, Iran. Tel: +98 (411) 334-1315, Fax: +98 (411) 334-4798, E-mail: jelvehgri@tbzmed.ac.ir

the gastrointestinal environment and may lengthen contact of nanospheres with the epithelium that may be enough to increase the bioavailability of certain drugs (12-16). In the present investigation, VCM was incorporated in Eudragit RS-100 nanoparticles, with the aim of ameliorating intestinal permeability. Loading of VCM, a hydrophilic antibiotic, into RS-100 microparticles can be problematic owing to its high hydrophilicity . The most used technique to encapsulate hydrophilic molecules is the double (water-in-oil-in-water, W/O/W) emulsification method, followed by solvent extraction/evaporation (17). Aqueous solution of the hydrophilic compound is first emulsified in organic solution of the polymer. The primary emulsion is then poured into a large volume of water with or without surfactant. The double emulsion technique has fairly good encapsulation efficiency for hydrophilic compounds; however, particle size is usually larger than with single emulsion technique (18). Multiple emulsions of the W/O/W type are excellent candidates for controlled and sustained release of hydrophilic drugs due to the existence of a middle oil layer that accomplishes as a liquid membrane (19).

However, there have been no reports on preparing VCM nanoparticles using RS-100 and assessing their intestinal permeability. One of the most used classic techniques in the study of intestinal absorption of compounds has been the single-pass intestinal perfusion (SPIP) model, which provides experimental conditions nearer to what is encountered following oral administration (12-16). SPIP is the most used classic technique employed in the study of intestinal absorption of compounds in which a non-absorbable marker such as phenol red is used to adjust the water flux (20). SPIP proposes a simple and relevant method of permeability evaluation and coordinates very much with the true absorption properties in human beings (21). The applicability of the method is assessed by testing the physiological function of the rat intestine during perfusions. This technique has lower delicacy to pH variations and it maintains an intact blood supply to the intestine (12-16). The objective of this study was improving intestinal permeation. It sounds alternative formulations are needed to extend the time over which the VCM intestinal level remains high enough and therefore enhance the oral performance of this suitable antibiotic. Reversed-phase high performance liquid chromatography (HPLC) is the most credible approach to the assay (22). In this study, we identified P_{eff} and oral fractional absorption (F_a) of VCM in the rat intestine.

Materials and Methods

Materials

Vanko® was obtained from Jaberebnehyan Pharmaceutical Company, Iran. Eudragit RS-100 was purchased from RÖhm Pharma GMBh, Weiterstadt, Germany. Poly vinyl alcohol (PVA) with molecular weight of 95000 Da was provided byAcros Organics, Geel, Belgium. Dichloromethane, methanol, glacial acetic acid, triethanolamine, hydrochloric acid, potassium chloride, acetone, sodium chloride, sodium hydrogen phosphate (dibasic), potassium dihydrogen phosphate were received from Merck, Darmstadt, Germany. Dialysis bag (10,000 Da) for invitro release studies was procured from Biogene (Mashhad, Iran). Male Wistar rats were purchased from the animal house of Tabriz University of Medical Sciences. All other reagents used were analytical grade.

Preparation of nanoparticles

VCM- Eudragit RS100 nanoparticles were prepared by the W1/O/W2 modified solvent evaporation method Using different ratios of drug to polymer (1:1, 1: 2 and 1: 3). Briefly, 5 ml of aqueous internal phase was emulsified for 120 s in 20 ml of methylene chloride (containing 100, 200 and 300 mg Eudragit RS-100) using homogenizer with 24000 rpm. This primary emulsion was added into 25 ml of a 0.2% PVA aqueous solution while stirring using a homogenizer for 3 min, immersed in an ice water bath, to create the water in oil-in-water emulsion. Approximately five ml of NP suspension was prepared after solvent evaporation under reduced pressure (Evaporator, Heidolph, USA). Nanoparticles were separated from the bulk suspension by centrifugation (Hettich universal 320R, USA) at 21,460×g for 20 min. The supernatant was kept for drug assay as described later and the precipitated nanoparticles were collected by filtration and washed with three portions of 30 ml of water and were redispersed in 5 ml of purified water before freeze-drying. After lyophilization, the dried nanoparticles were resuspended in 50 ml of Phosphate buffered saline (PBS)12hrs before perfusion. Blank nanoparticles (without drug) were prepared under the same conditions without drug (23, 24).

Nanoparticle size

A laser light scattering particle size analyzer (SALD-2101, Shimadzu, Japan) was used to determine the particle size of the drug, polymer and nanoparticulate formulations. Samples were suspended in distilled water (nanoparticles and polymer) or acetone (drug) in a 10 cm cuvette and stirred continuously during the particle size analysis.

Zeta potential measurement

The zeta potential of a nanoparticle is commonly used to characterise the surface charge property of nanoparticles. It shows the electrical potential of particles is influenced by the composition of the particle and the medium in which it is dispersed. Currently principal technique involved in zeta potential determination is laser doppler anemometry. Nanoparticles with a zeta potential above (+/-) 30 mV have been shown to be stable in suspension, as the surface charge prohibits aggregation of the particles (25). These might result in stronger repulsive

interactions among the particles, and hence, higher stability of the particles is achieved (26). The zeta potential can also be used to determine whether a charged active material is encapsulated within the centre of the nanocapsule or adsorbed onto the surface (25). Zeta potential was measured by Zetasizer (Malvern instruments, England). The samples were diluted with 0.1 mM NaCl solution at a series of pH values in order to maintain a constant ionic strength and measured in automatic mode. Each sample was repeated measured three times and the values reported were the mean value for two replicate samples. Zeta potential is an important consideration, since membranes often bear (negative) surface charge. Therefore, to enhance the particle cellular uptake, the surface of particles might be adjusted by positively charged surface functional groups (27). Zeta potential measurement is made to optimize formulation parameters and to make predictions regarding the storage stability of the colloidal dispersion (28).

Determination of drug loading (DL), encapsulation efficiency (EE) and production yields (PY)

DL can be done by two methods:

• Incorporating at the time of nanoparticles production (incorporation method)

• Absorbing the drug after formation of nanoparticles by incubating the carrier with a concentrated drug solution (adsorption /absorption technique) (29). For determinating of DL, freeze-dried nanoparticles was dissolved in a known volume of methanol.The amount of VCM was quantified by measuring the absorbance at 279.6nm . Another method for determining of DL is measuring the amount of non-entrapped VCM in the external aqueous solution. The results of these two methods were consistent. Ideally, a successful nanoparticulate system should have a high DL capacity thereby reduce the quantity of matrix materials for administration (29). DL and EE very much depend on the solid-state drug solubility in matrix material or polymer (solid dissolution or dispersion), which is related to the polymer composition, the molecular weight, the drug polymer interaction and the presence of endfunctional groups (ester or carboxyl) (30-32). The EE of VCM in RS-100 nanoparticles was determined spectrophotometrically (UV-160, Shimadzu, Japan) at 280.2 nm by measuring the amount of non-entrapped VCM in the external aqueous solution (indirect method) before freeze-drying. The external aqueous solution was procured after centrifugation of the colloidal suspension for 20 min at 21,460×g at 25°C. A standard calibration curve was plotted with the VCM solution (aqueous solution of 0.2% PVA). The EE (%) was calculated according to the following equation:

encapsulation efficiency (%) = (actual drug content in nanoparticles/theoretical drug content) × 100.

Independently of the drug-to-polymer weight ratio, the **PY** % (expressed as practical mass *100/Theoretical mass(polymer+drug)) are relatively high (33). All of the experiments were performed in triplicate.

X-ray diffraction, Infrared spectroscopy and differential scanning calorimetry (DSC) studies

Powder X-ray diffraction (XRD) patterns of the pure drug and polymer and also nanoparticles were obtained using an X-ray diffractometer (Siemens D5000, Munich, Germany) equipped with a graphite crystal monochromator (CuKα) (a voltage of 40 KV and a current of 20 mA) as X-ray source to observe the physical state of the drug in the microspheres. The scanning rate was 6°/min over the range of 5-70° and with an interval of 0.02°. FTIR spectra were recorded to assess the compatibility of the drug and polymer (34).The infrared (IR) spectra of VCM powder, physical mixture of drug and polymer, and prepared nanoparticles were recorded on an IR-spectrophotometer(range 450-4000 cm^{-1}) (BomemHartmann & Brann, Canada) by the KBr pellet technique. Samples were prepared in KBr disks (2 mg sample in 20 mg KBr). Sample analysis were carried out by the E2 OMNIC software for analysis. With reasonable intensity, the spectrum was saved for further analysis at 1 cm^{-1} resolution. Differential scanning calorimetry (DSC) was employed to identify any changes in the thermal behavior of VCM nanoparticles compared to original materials. DSC was also used to study the thermal behavior of the granules of the raw material and the film of polymers (35). DSC analysis was performed using a DSC-60 calorimeter (Shimadzu, Japan). The instrument was equipped with a TA-60WS thermal analyzer, FC-60A flow controller and TA-60 software. Samples of VCM, polymer, physical mixture and agglomerates were located in an aluminum crucible and were heated ranging 25-300 °C at a scanning rate of 10 °C/min under a nitrogen atmosphere. A similar pan contain indium was used as reference.

Dissolution study

The in vitro release of the drug from the polymeric nanoparticles was studied by the dialysis bag diffusion technique and under sink conditions for all nanoparticles formulations. The dialysis bag retained nanoparticles and allow the diffusion of the drug immediately into the recipient compartment (36). A set amount of nanoparticles (20 mg drug) was added to 200 ml dissolution medium (PBS, pH 7.4), an in vitro dissolution medium imitates the pH and salt concentrations in the body, preheated and maintained at 37±1 °C in a water bath, then stirred at 100 rpm. Then 3 ml of the medium were withdrawn at preset times by an automatic sampling system (Erweka DT 70, Erweka GmbH, Heusenstamm, Germany), (0.5, 1, 2, 3, 4, 5, 6, 8, 12 and 24 hrs). Each sample was centrifuged at 21,460×g for 10 min. An equal volume of fresh medium was added after each sampling. The amount of

VCM in the release medium was determined by UV at 279.8 nm (37). Each experiment was performed in triplicate.

Calibration curve

Accurately weighed quantities of VCM hydrochloride were dissolved in a PBS, pH 7.4 to acquire solutions with known concentrations in the range of 31.25–500µg/ml. The spectra of these solutions were registered against the same medium, and absorption was measured in the 279.8 nm by spectrophotometer. Each experiment was performed in triplicate, After that the calibration graph was plotted.

Perfusion solution

The perfusion solution was prepared by dissolving 7g NaCl, 0.2g KCl, 1.44 g Na2HPO4(anhydrous) and 0.24g KH_2PO_4 in one liter of distilled water. The pH of prepared PBS was 7.4. preparatory experiments showed that there was no considerable adsorption of the compounds on the tubing and syringe. Primary stock solution of drug, phenol red and nanoparticles was prepared in PBS (15). Then it was diluted to 200-400µg/ml to make a working solution and standards for calibration curves and quality control samples were prepared using serial dilution of working solution in PBS. This range was selected based on the concentration that were going to used in animal studies. All standards were freshly prepared for every study.

In situ permeation studies

Adult male Wistar rats (200-250 g) were housed in air conditioned. Rats were maintained on 12 h light- dark cycle and fasted 12-18 h before experiment. However drinking water was accessible. Rats were divided into control and test groups. In each group three concentration levels of VCM (200, 300 and 400 µ g /ml) were used in separate experiments. Rats were anaesthetized using an intraperitoneal injection of pentobarbital (50 mg/kg) and placed on a heated pad to keep normal body temperature. A small midline cut was made in the abdomen and a 10 cm section of the small intestine was identified and cannulated. Care was taken to handle the small intestine gently and to minimize the surgery in order to maintain an intact blood reserve. The entire surgical area was then covered with Parafilm to reduce evaporation. Blank perfusion buffer was infused for 10 min by a syringe pump (Palmer, England) followed by perfusion of different concentrations (200, 300, 400 µ g/ml) of VCM (prepared from its powder or its nanoparticles) at a flow rate of 0.2 ml/min for 80 min. Outlet samples were collected at appropriate intervals (40, 50, 60, 70, 80 min with half hour lag time for balance) in microtubes. The volume of sample for each time interval was 2 ml. When the experiment was completed, the length of segment was measured and the animal was euthanatized with a cardiac injection of overdose of sodium pentobarbital. Samples were stored at -20 °C until analysis. Samples from perfusion study were filtered and directly injected onto HPLC column. Effective permeability coefficients (P_{eff}) were calculated from the steady-state concentrations of compounds in the collected perfusate, which is considered to be reached when the concentration level of phenol red was at the steady state level. It was reached about 30 min after the beginning of the perfusion, which is approved by plotting the ratio of the outlet to inlet concentrations (corrected for water transport) versus time. The intestinal net water flux (NWF, µ l/h/cm) was calculated according to following equation:

$$NWF= Qin(1-(Ph.redout/Ph.redin))/l$$

Where (Ph.red(in)) and (Ph.red(out)) are the inlet and outlet concentrations of phenol red. A negative net water flux showes loss of fluid from the lumen to the serosal side. A positive net water flux indicates secretion of fluid into the segment (38). P_{eff} was calculated using the following equation according to the parallel tube model:

$$P_{eff}= -Qln(Cout/Cin)/2\pi r\ell$$

In which Cin is the inlet concentration and Cout is the outlet concentration of compound which is corrected for volume change in segment using phenol red concentration in inlet and outlet tubing. Q is the flow rate (0.2 ml/min), r is the rat intestinal radius (0.18 cm) and ℓ is the length of the segment (39). In all animal studies "Guide to the care and use of experimental animals" by Canadian Council on Animal Care, was followed (40). The P_{eff} for passively absorbed compounds is on average 3.6 times higher in humans compared to rats. Solutes with carrier-mediated absorption deviate from this relationship, which indicates that an absolute scaling of active processes from animal to man is difficult, and therefore needs further investigation. The oral fractional absorption of drugs after oral administration in humans (fa) can be estimated from this equation:

$$Fa=1 - e^{-(2.P\ eff,man\ .tres\ /r.f)}$$

Where t_{res} and r are the average small intestinal transit time and radius in humans, and are assumed to be 3 hrs and 1.75cm, respectively. The relationship between our human P_{eff} and Fa (from in vivo pharmacokinetic studies), expressed as correction factor *f* was determined by non- linear regression. The *f*-value was then used for simulation and prediction of Fa in vivo in man. The *f* is approximately 2.8 (38).

Chromatographic conditions

Perfusion samples were analyzed using a modified reversed-phase high performance liquid chromatography (RP-HPLC) method. Reverse-phase

HPLC was achieved at room temperature. HPLC system containing an autosampler (Hewlett-Packard 1050 Series), quaternary pump thermostat, variable-wavelength UV–Vis spectrophotometer detector (all from Hewlett-Packard, Waldbronn, Germany). The analytical methodology was demonstrated for specificity, accuracy, precision and sensitivity. Wavelength ultraviolet spectrophotometric detector (Knauersmartline 2500) set at 430 nm and 254 nm for phenol red and VCM, respectively. EZChrom Elite version 2.1.7 was used for data attainment, data reporting and analysis. The mobile phase for VCM analysis consisted of 30% (v/v) methanol and 70% (v/v) of glacial acetic acid aqueous solution (0.75%) adjusted to pH 5.5. For phenol red analysis the mobile phase consisted of 45% (v/v) KH2PO4 0.05 M and 55% (v/v) methanol adjusted with triethanol amine to pH 2.6. The mobile phases were filtered with a 0.45 mm pore size cellulose membrane filter, and degassed before use. Analytical column used for chromatographic separations was packed with Adsorbosil ODS C18 (250 × 4.6 mm) 5 µm with precolumn. 20 µl of samples or calibration standards were injected directly onto the column and were eluted with a gradient consisting of phosphate buffer. Until termination of the run at 20 min, the flow rate was 1 ml/min. The system was equilibrated for 20 min under the starting conditions before injecting the next sample. Under the mentioned conditions the retention times for VCM and phenol red were 5 min and 13.8 min, respectively. Runs contained quality control samples (QC) at three concentrations levels. Calibration curves were acquired by plotting the phenol red and VCM peak area against their concentrations in standard solutions (41, 42). Each determination was carried out in triplicate (SD within 0.09).

Results

Micromeritics properties

Encapsulation efficiencies of VCM nanoparticles are reported in Table 1. It is evident from Table 1 that the encapsulation efficiency was affected by the ratio of drug:polymer. Mean particle diameter and production yield of the different nanoparticles are also shown in Table1. The encapsulation efficiency of the drug depended on the solubility of the drug in the solvent and continuous phase. Youan & etal. have been reported Similar observation. VCM is insoluble in organic solvents used to dissolve the polymer and thus cannot migrate from the internal into the external aqueous phase via diffusion through the organic polymer solution. Entrapment efficiency of polypeptides was increased by enhancing the viscosity creators (43). Despite the hydrosolubility of VCM, favoring the leakage of the drug into the external aqueous phase, entrapment efficiencies were rather high. It is assumed that VCM is localized at the interfaces (either internal water in oil or external oil in water). Therefore a considerable amount of drug is supposed to be adsorbed at the outer surface. In addition, the elimination of the organic solvent under reduced pressure favors its fast evaporation followed by the polymer precipitation, thus reducing the movement of the drug to the external phase. At the ratio of drug to polymer 1:3 the amount of drug entrapment was 23.69% which was very near to the theoretical value (25%).

The particle size data show that prepared nanoparticles were of submicron size and of small polydispersity, which indicated a relatively narrow particle size distribution. An increase in particle size from 362 nm to 499 nm with a decrease in the theoretical drug loading was also observed (Table 1). As it can be seen, the particles size are increased with increasing polymer amount (44, 45). When the dispersed phase with higher viscosity was poured into the dispersion medium, bigger droplets were formed with larger mean particle size. It has also been reported that the particle size increases with increasing the content in hydrophobic polymer. It can be assigned to that fact that with the higher diffusion rate of non-solvent to polymer solution the smaller size of nanocapsules is easily obtained (46). A volume-based size distribution of drug, polymer, and drug-loaded nanoparticles indicated a log–probability distribution. The increase in drug content of the nanoparticles with increased theoretical drug loading has emerged in the decreased particle sizes displayed (p<0.05).

Table1. Effect of drug: polymer ratio on drug loading efficiency, production yield, particle size zeta potential and polydispersity index of vancomycin nanoparticles

Formulation code	Drug: polymer ratios	Production yield (%±SD)	Theoretical drug Content (%)	Mean drug Entrapped (%±SD)	Drug loading efficiency (%±SD)	Mean particle Size (nm±SD)	Zeta Potential (mV±SD)	Polydispersity Index (PDI)
F_1	1:1	96.38 ±1.65	50	30.25 ±1.04	63 ± 2.19	362±29.26	18.1±8.82	0.0099
F_2	1:2	97.84 ±1.54	33.33	29.79 ±1.12	89.37±2.36	430±31.94	25.7±9.72	0.0055
F_3	1:3	98.35 ±1.87	25	23.69 ±1.02	94.76± 1.95	499 ± 110	24.1±7.17	0.0034

The average yield of 97% is in the normal range does not indicate any unexpected vanishment of products.
Zeta potential is the potential difference the dispersion medium and stationary layer of fluid attached to the dispersed particles. The significance of zeta potential is that its value can be pertained to the stability of colloidal dispersion (28) . The zeta potential indicates the degree of repulsion between near, similarly charged particles in dispersion. As to the zeta potential, the larger its absolute value is, the more likely the suspension is to be stable, since the charged particles repel one another and thus defeat their natural tendency to aggregate (47). The zeta potential measurements showed posetively-charged particle surfaces, varying from 18.1 to 25.7mV. Drug-loaded nanoparticle indicated positive charge, because VCM is cationic drug and changed the charge of nanoparticles. All the gained values were then acceptable and favoring a good stability. The zeta potential of three nanosphere formulations is shown in Table 1. Blank nanoparticles like nanoparticles had a positive charge (15.7 mV).

DSC Analysis

DSC was employed to study the crystallinity of nanoparticles. DSC studies were carried out to confirm compatibility (48). The thermal behavior of drugs, physical mixture of drug and polymer, and formulations was studied. Any sudden or forceful change in the thermal behavior of the drug or polymer may indicate a possible drug-polymer interaction (49). The endothermic peak of the pure drug was observed at about 82.10°C (Figure 1) and Eudragit RS100 showed an amorphous state. The physical mixture of VCM and RS100 showed nearly the same thermal behavior as the individual components, indicating that there was no interaction between the drug and the polymer in the solid state. Indeed, in the thermogram of the nanoparticles containing Eudragit RS, there was endothermic peak at 219.92°C which accords to the melting point of drug in the nanoparticles. In the DSC curve of physical mixture of drug and polymer, and formulations F1, F2 and F3, the characteristic peaks of drug were observed. The results showed that there is no incompatibility between drug and polymers.

Powder X-ray diffractometry

XRPD is a powerful tool to identify any changes in crystallinity of drug (polymorphism) (50). Comparison of the X-ray diffraction patterns of VCM and nanoparticles prepared with RS-100 (Figure 2) showed no remarkable reduction in the peak intensities, suggesting that the expanse of VCM crystallinity was not reduced by the polymer. The X-ray diffraction patterns of pure drug and Eudragit RS showed that the pure drug is crystalline in nature (Figure 2). As shown in Figure 2, Eudragit RS100 is a typical form of amorphous materials, whereas the pure drug showed the diffractographic profile of a crystalline material. When the nanoparticles were prepared with different polymer/drug ratios (F1, F2 and F3) it is clear that the nanoparticles with lower polymer concentration showed similar peaks as the blank nanoparticles. At high concentration of polymer and low concentration of drug some of the distinguishing peaks for VCM are detectable but with very low intensity due to the presence of lower concentration of drug in the sample in comparison with pure VCM sample. This confirms the results obtained from DSC.

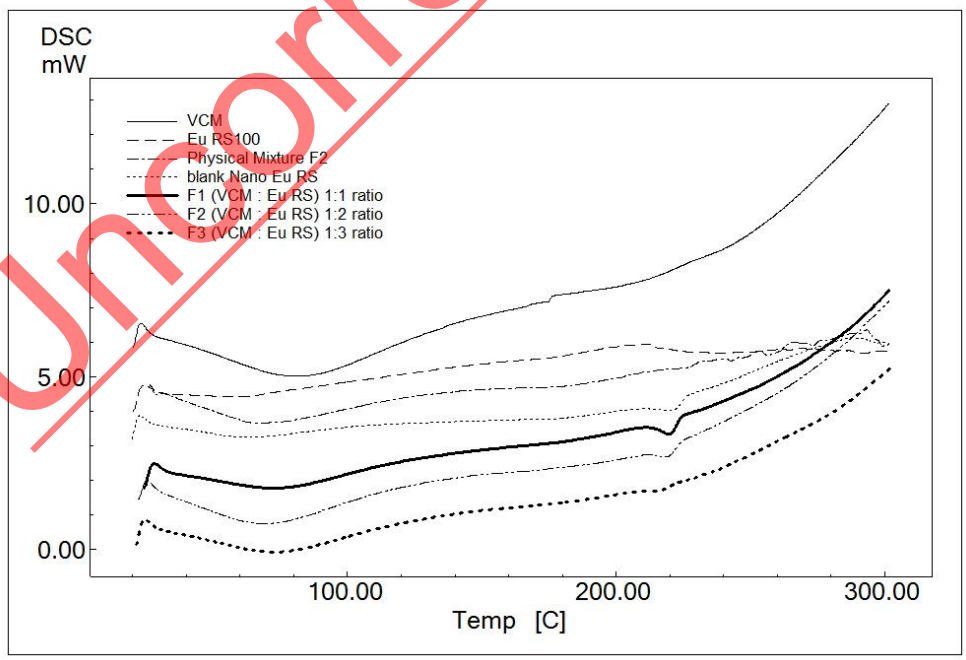

Figure1. DSC thermogram of the VCM; RS100; PVA; physical mixture F_2; blank nanoparticles, VCM nanoparticles formulations as F_1, F_2 and F_3.

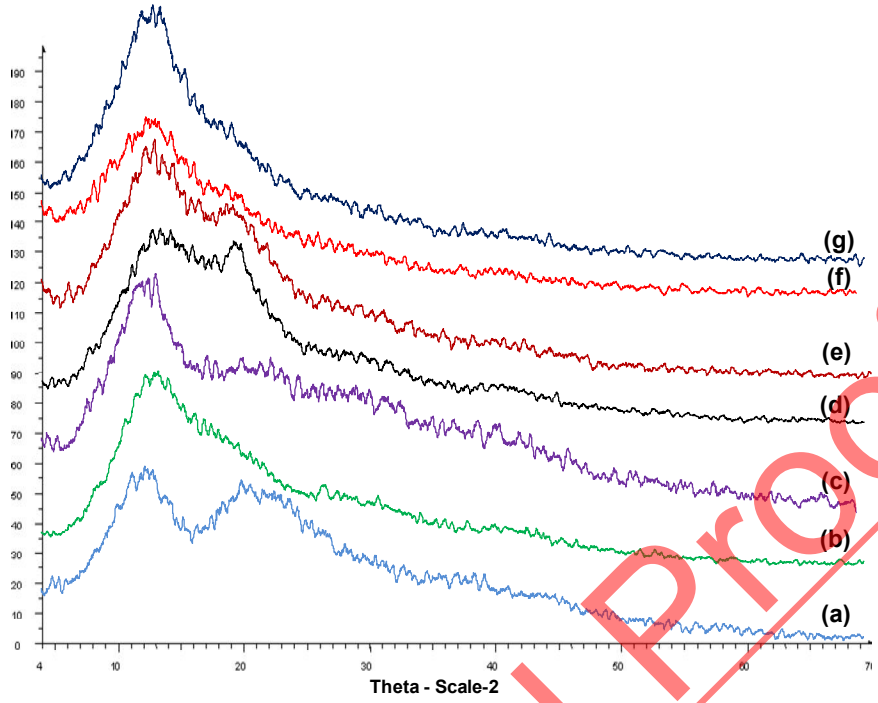

Figure2. X-ray diffraction a) VCM; b) RS100; c) Physical Mixture F2; d) blank nanoparticles; e) VCM : RS100 (1:1); f) VCM : RS100 (1:2); g) VCM RS100 (1:3).

FTIR Studies

The FTIR spectra of VCM, VCM-loaded RS-100 nanoparticles, physical mixture F_2 (1:1), and the individual components are portrayed in Figure 3. The FTIR of VCM showed phenolic OH at 3257.39 cm^{-1}, aromatic C=C stretching at 1652.7 cm^{-1} and C=O stretching at 1503.48 cm^{-1}. The peaks in the range between 2800 and 3100cm^{-1} pertain to the C—H stretching bands, the peak in the range between 1650 and 1800cm^{-1} is due to the C=O stretching vibrational groups, and the peak in the range between 1350 and 900 cm^{-1} corresponds to the C—O stretching vibration mode. The peaks within 2950–3000 cm^{-1} assigned to the stretching vibrations of CH2 and CH3, the peak at 1763 cm^{-1} conforms the C=O ester vibration, and the peak at 1153 cm^{-1} is fitted with the C—O ester vibration, respectively. Eudragit RS-100 has C=O stretching band at 1734.2 cm^{-1}. nanoparticles F1, F2 and F3 have C=O stretching band at 1731.2, 1733.7, 1733.96 cm^{-1}, respectively (Figure 3). After VCM was encapsulated into the nanoparticles, the characteristic peaks for VCM showed by the stronger intensity peaks for of matrix materials. On the other hand, the C=O stretching bands of VCM in polymeric systems were merged, thus leading to a peak shifting from 1731.2 cm^{-1} to 1733.96 cm^{-1} (51). The bands observed for nanoparticles spectrum showed similar unique peaks but with smaller intensity due to low concentration of drug in nanoparticles. No differences in the positions of the absorption bands were observed in spectra of the VCM physical mixture with RS-100, indicating that there are no chemical interactions in the solid state between the drug and the polymer. This suggests that there was no new chemical bond constructed between these functional groups in the drug and the polymer after preparing the nanoparticles and the results confirmed that the drug is physically dispersed in the polymer. FTIR investigations confirmed the compatibility of VCM and RS100.

In vitro release study

The mean cumulative release (%) versus time curves is shown in Figure 4. The rate of dissolution of physical mixture is quite fast, and more than 96% drug is dissolved in about 30 min and 100% by 60 min. The drug release from the nanoparticles manifested to have two components with an immediate release of about 10.78-12.27% at the first sampling time of 30 min. This was followed by a slower exponential release of the remaining drug over the next 6-8 h. The in vitro VCM release profiles from drug-loaded nanoparticles are also illustrated in Figure 4. Furthermore, Figure 4 clearly presentes that the rate of drug release from the nanoparticles depended on the polymer concentration in the system. A similar relationship was observed between polymer content and drug release rate from prepared nanoparticles. By decreasing the concentration of the polymer in the system, an increase was shown in the release rate of VCM. The difference was also not significant ($p > 0.05$) for 0.5 or 24 h. It is offered that a reduced diffusion path and increased tortuosity may have retarded the drug release rate from the matrix at the presence of polymer matrix.

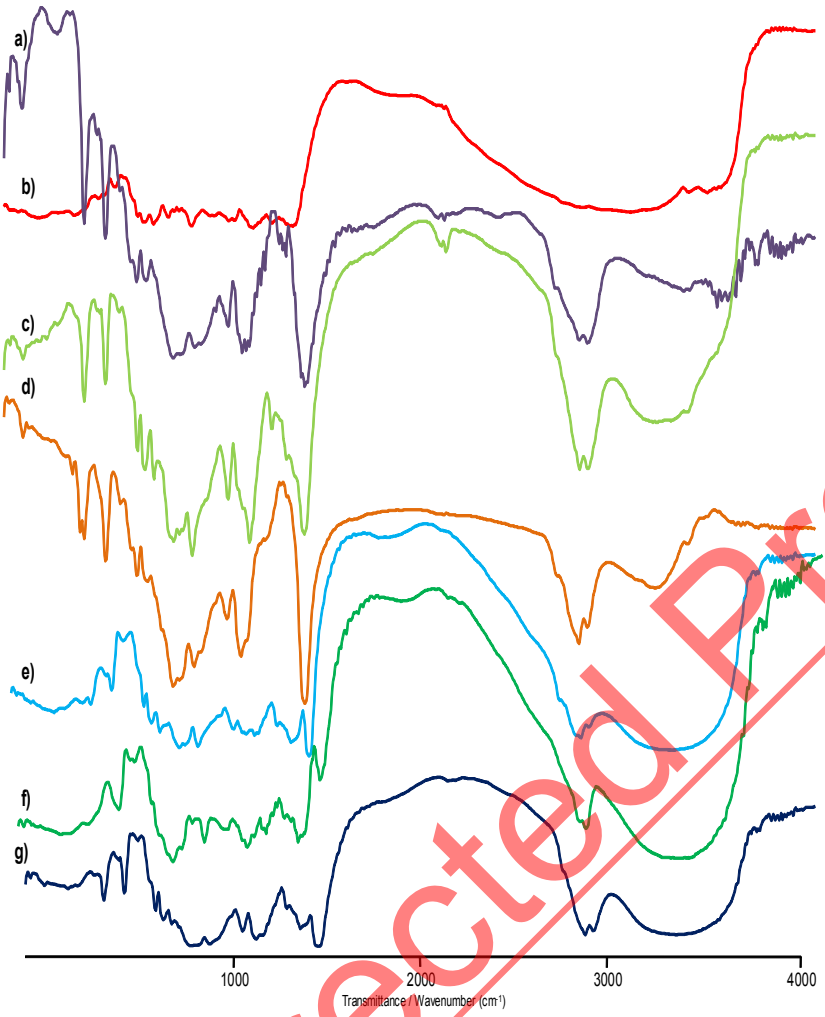

Figure3. FTIR spectrum; a) RS100; b) VCM; c) Physical Mixture F_2; d) blank nanoparticles; e) VCM : RS100 (1:1), f) VCM : RS100 (1:2), g) VCM : RS100 (1:3).

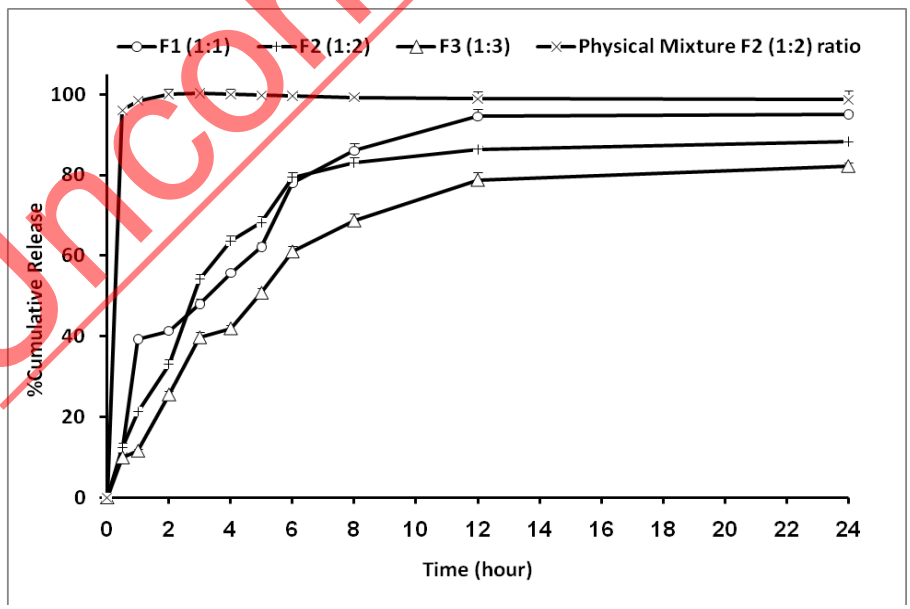

Figure4. Cumulative percent release of VCM nanoparticles prepared with different drug-to-polymer ratio and physical mixture F_2.

Nanoparticles containing 1:1 (F_1) released the drug more rapidly, wherease F_3 exhibited a relatively slower drug release profile. F_1, F_2 and F_3 nanoparticles showed higher dissolution efficiency of 81.44, 76. 25 and 66. 37%, respectively. Physical mixture of drug and polymer exhibited higher release in comparison with microspheres ($p< 0.05$) (Table 2 & Figure 4). The presence of Eudragit RS100 in the matrix of nanoparticles caused a slower and more advancing release of VCM during the time of the experiment (52). The lowest dissolution efficiency was showed for F3 (66. 37%) and dissolution efficiency of the physical mixture was 98.03% ($p< 0.05$). The value of $t_{50\%}$ varies between 2.24 (F_2 formulation) to 4.85 h (F_3 formulation). The results of difference factor (f_2) observed that there is no similarity between the release profiles of nanoparticle formulations and physical mixture (Table 2). The in vitro release profiles were fitted to various kinetic models (Higuchi, first-order, zero-order, Peppas, Hixson crowell, square root of mass, three second root of mass, weibull, linear probability and log- probability) in order to determine the mechanism of drug release (23). The dissolution rate constants were calculated from the slope of the respective plots and high correlation was observed for the Peppas models (Table 3). The data obtained were also put in Korsemeyer-Peppas model in order to find out n value, which particularizes the drug release mechanism. The n value of nanospheres of different drug to polymer ratio was between 0.392-0.569, indicating that the mechanism of the drug release were diffusion controlled.

Table2. Comparison of various release characteristics of vancomycin from different nanoparticle formulations and physical mixture

Formulation	[a]$t_{50\%}$ (h)	[b]DE	[c]$Q_{0.5}$	[d]Q_{24}	Difference Factor (f_1)
F_1	3.25	81.44	11.44±0.99	95.03±2.17	38.11
F_2	2.24	76.25	12.27±1.25	88.27±0.77	40.52
F_3	4.85	66.37	9.95±0.49	82.23±0.78	52.55
Physical mixture	0.26	98.03	96.10±0.43	98.70±0.52	0.04

[a]dissolution time for 50% fractions. [b]Dissolution Efficiency. [c]amount of drug release after 0.5h.[d] amount of drug release after 24h

Intestinal permeability and oral fractional absorption data

In any in situ intestinal perfusion technique it is necessary to determine the magnitude of volume changes of the solution in the gut lumen during an experiment. For this purpose phenol red dye (200 µ g/ml) was added to drug solution in each experiment. Phenol red was used as a non-absorbable marker to detect gain or loss of water by the lumen. The determined mean P_{eff} values for different concentrations of vancomycin and its nanoparticles in PBS, oral fractional absorption and also the mean net water fluxes in the SPIP technique are listed in Table 4.

Discussion

The organic phase (O) behaves as a barrier between the two aqueous compartments. To control the methylene chloride elimination time and rate, we used a rotary evaporator method. Thus, the transfer of the drug into the external phase (W_2) was hampered. The particle formation itself is based on coacervation. The solvent is extracted from the polymer containing organic phase because of its initial diffusion into the continuous W_2 phase, motivating phase separation of the polymer. The organic solvent is eliminated by two steps; firstly by extraction and secondly by evaporation. In general, the solvent removal rate directly affects the encapsulation efficiency of a drug(53, 54) because the slow membrane formation rate may reduce the encapsulation efficiency as a result of improving the chances of drug molecules to be diffused out from the inner W_1 phase to outer W_2 water phase (54, 55). It is deduced that rapid membrane formation is an important criterion preventing the leakage of VCM to the W_2 phase. Generally, PVA is used as a surfactant in the $W_1/O/W_2$ emulsion method to comprise it onto the surface of RS-100 particles, thereby lowering the surface tension between the RS-100 surface and the W_2 phase (54, 56). However, because PVA cannot be washed away absolutely, it remains on the surface of RS-100 (54, 57). PVA concentration in the external water phase is known to be a important factor to influence the size of nanoparticles (43). The low drug incorporation efficiency may be ascribed to the water soluble nature of VCM hydrochloride. This led to its rapid partitioning into the aqueous phase and accordingly decreased entrapment into the nanoparticles during polymer deposition. The decreased drug entrapment with increasing theoretical drug loadings is due to an enhanced drug exudation into the aqueous phase at high loadings.

Table 3. Fitting parameters of the *in vitro* release data to various release kinetic models for nanoparticles

	ORDER	RSQ	Slope	intercept	MPE%	K
F_1	Zero order	0.627	0.036	0.341	3.1E+14	0.036
	First order	0.891	-0.152	-0.314	2.5E+14	-0.152
	Second order	0.950	1.320	-2.217	1.7E+15	1.320
	Higuchi	0.876	0.220	0.103	9.3E+13	0.220
	Peppas (Power Low)	0.999	0.569	-1.404	15.8656	1.767
	Hixson-Crowell	0.816	0.029	0.122	2.9E+14	0.029
	Square root of mass	0.770	0.034	0.184	3E+14	0.034
	Three-seconds root of mass	0.722	0.036	0.242	30.1957	0.036
	weibull	0.998	0.583	-0.857	15.6951	0.230
	Linear-probability	0.323	0.197	-1.446	5.5E+13	0.197
	Logarithmic-probability	0.911	0.160	0.198	59.8762	0.160
F_2	Zero order	0.543	0.034	0.335	3046748	0.034
	First order	0.714	-0.094	-0.459	3344353	-0.094
	Second order	0.855	0.353	0.497	3018450	0.353
	Higuchi	0.819	0.212	0.098	889793	0.212
	Peppas (Power Low)	0.995	0.393	-1.218	32.3218	1.481
	Hixson-Crowell	0.656	0.022	0.138	3271499	0.022
	Square root of mass	0.627	0.027	0.197	3222189	0.027
	Three-seconds root of mass	0.598	0.031	0.248	3167227	0.031
	weibull	0.986	0.410	-0.744	33.1694	0.163
	Linear-probability	0.339	0.142	-1.043	1349436	0.142
	Logarithmic-probability	0.868	0.155	0.066	61.8763	0.155
F_3	Zero order	0.686	0.034	0.226	2054809	0.034
	First order	0.834	-0.077	-0.238	1926127	-0.077
	Second order	0.925	0.213	0.102	841078	0.213
	Higuchi	0.905	0.199	0.016	149265	0.199
	Peppas (Power Low)	0.994	0.414	-1.515	30.4708	1.512
	Hixson-Crowell	0.788	0.019	0.080	2014231	0.019
	Square root of mass	0.763	0.025	0.119	2037665	0.025
	Three-seconds root of mass	0.738	0.029	0.157	2050986	0.029
	weibull	0.986	0.427	-1.179	34.4088	0.063
	Linear-probability	0.377	0.139	-1.359	791204	0.139
	Logarithmic-probability	0.871	0.155	-0.301	66.9204	0.155
Physical mixture	Zero order	0.081	0.012	0.828	7526441	0.012
	First order	0.016	0.072	-6.560	9078026	0.072
	Second order	0.042	-8796.400	153390.990	9090842	-8796.367
	Higuchi	0.261	0.112	0.669	6082596	0.112
	Peppas (Power Low)	0.982	0.508	-0.724	25.1718	1.662
	Hixson-Crowell	0.032	0.007	0.722	8895392	0.007
	Square root of mass	0.060	0.010	0.781	8656034	0.010
	Three-seconds root of mass	0.074	0.011	0.808	8326018	0.011
	weibull	0.973	0.574	0.991	4.88962	5.616
	Linear-probability	0.022	0.053	1.901	8830365	0.053
	Logarithmic-probability	0.837	0.281	2.517	10.1867	0.281

Table 4. Permeability coefficients and oral fractional absorption determined in rats for test and control groups

Group	C_{in}	Mean Puff ($\times 10^5$ cm/sec)	oral fractional absorption	Mean NWF (ml/min/cm)
control	200	6.11(± 2.66)	0.37(± 0.17)	0.0003(± 0.0002)-
	300	3.87(± 2.45)	0.53(± 0.09)	0.0006(± 0.0003)
	400	2.54 (± 1.64)	0.28(± .012)	0.0004(± 0.0001)
test	200	17.88 (± 2.61)	0.45(± 0.15)	0.0005(± 0.0002)-
	300	16.63(± 2.98)	0.77(± 0.13)	0.0004(± 0.0002)
	400	15.75(± 4.47)	0.42(± 0.20)	-0.0006(± 0.0003)

Zeta potential results (Table 1) showed that drug-loaded formulations carried a positive charge, which assists particle stability because the repulsive forces prevent aggregation with aging. It has been reported that the positive charge of RS-100 nanoparticles is due to positive charge of VCM (58) , because VCM is cationic drug and changed the charge of nanoparticles. Drug-free RS-100 nanoparticles had a positive surface charge of 15. 7 mV, which can be attributed to the presence of carboxyl groups and quaternary ammonium of the polymer on the nanoparticles (30). Zeta potential measurements showed a insignificant increase in positivity (from 18.1 mV to 25.7 mV) with an decrease in theoretical drug loadings. These findings are concuring to what was expected, for instance a decrease in the surface positivity due to interaction of carboxyl groups and the cationic drug on the particle surface. The increase in nanoparticle size with decreases in the theoretical drug loading of VCM (Table 1) may possibly have influenced the surface charge of the RS-100 nanoparticles (59). From the data it is obvious that all the formulations are almost unstable in the colloidal state. This indicates that the particles should not be stored in a liquid suspension form and rather they should be stored in a lyophilized state (59) .The rapid initial release of VCM was probably due to the drug which was adsorbed or near to the surface of the nanoparticles and the large surface to volume ratio of nanoparticle geometry because of their size (30). It may also be due to the water soluble nature of VCM. The exponential delayed release may be attributed to diffusion of the dissolved drug within the RS-100 core of the nanoparticle into the dissolution medium. Similar observations were reported by other researchers working (60, 61). Loading of VCM into the nanoparticles prompts to a modification of in vitro drug release, depending on their combination . The data obtained were also put in Korsemeyer-Peppas model in order to perceive the n value, which describes the drug release mechanism. The n value of nanospheres of different drug:polymer ratio was between 0.39-0.56, indicating that the drug release was diffusion controlled (Table 3). On the other hand, from the acquired results in rats it is demonstrated that the intestinal permeability oral fractional absorption of VCM is significantly increased using its nanoparticles in all three concentrations which were used ($P < 0.05$). The stable water fluxes and permeability coefficients in each perfusion, as a function of time, for tested compounds indicated that intestinal barrier function was maintained during the methodology. The intestinal permeability of VCM was determined to be in the range of 1.96 $(\pm 1.09)\times 10^{-5}$cm/sec to 4.66 $(\pm 1.32)\times 10^{-5}$ cm/sec in control groups. regardless, the drug permeability in test groups' intestinal segments which were perfused by VCM nanoparticles in PBS, ranged between 3.68 $(\pm 2.82)\times 10^{-5}$ cm/sec and 10.06 $(\pm 2.61)\times 10^{-5}$ cm/sec. There were statistical differences among the P_{eff} values in different concentrations. The maximum permeability, was seen at doses of 300 µg/ml. Therefore, it seems that the intestinal permeability of VCM is not concentration-dependent. The oral fractional absorption of VCM was determined to be in the range of 0.28 (±0.12) to 0.53 (±0.09) in control groups, while the test group was determined to be in the range of 0.42 (±0.20) to 0.77 (±0.13) (Table 4). In view of the hydrophilicity and high molecular weight of the peptidic drug, VCM, the higher intestinal permeability after nanonization is probable due to enhanced paracellular passage and endocytotic uptake, because the particles with small size are absorbed by intestinal enterocytes through endocytosis. Coating of VCM nanoparticles with PVA, a bioadhesive material, can also be a tactic to increase nanoparticle uptake by intestinal enterocytes. Nanoparticles coated with bioadhesive materials were contemplated to develop mucoadhesion. Adhesion of a carrier system to the mucus may improve residence time and drug contact with the underlying epithelium, thus increasing drug intestinal permeability which was demonstrated in the present study.

Conclusion

VCM-loaded RS-100 nanoparticles were successfully provided by using $W_1/O/W_2$ double-emulsion solvent evaporation method. Drug release from nanoparticles was more sustained than physical mixture. Moreover, the intestinal permeation and fractional absorption of VCM were improved using its nanoparticles and this may allow more efficient therapy compared to VCM formulations present in the market.

Acknowledgments

The financial support from biotechnology center, Tabriz University of Medical Sciences, is greatly acknowledged.

References

1. Robles-Piedras, A.L. and E.H. Gonz‹lez-Lpez. Therapeutic Drug Monitoring of Vancomycin. 2009.
2. Moellering Jr, R.C., Editorial: Monitoring Serum Vancomycin Levels: Climbing the Mountain Because It Is There? Clinical infectious diseases, (1994): 544-546.
3. Cook, F.V. and W.E. Farrar, Vancomycin revisited. Annals of internal medicine, 1978. 88(6): 813-818.
4. Bryan, C.S. and W.L. White, Safety of oral vancomycin in functionally anephric patients. Antimicrobial Agents and Chemotherapy, 1978. 14(4): 634-635.
5. Geraci, J., et al. Some laboratory and clinical experiences with a new antibiotic, vancomycin. 1956.
6. Florence, A.T., Nanoparticle uptake by the oral route: Fulfilling its potential? Drug discovery today: technologies, (2005) 2(1):75-81.
7. Yallapu, M.M., et al., Fabrication of curcumin encapsulated PLGA nanoparticles for improved therapeutic effects in metastatic cancer cells. Journal of colloid and interface science. 351(1): 19-29.
8. Kumar, G.S., et al., Synthesis and characterization of bioactive hydroxyapatite-calcite nanocomposite for biomedical applications. Journal of colloid and interface science, 2010. 349(1): 56-62.
9. Nouvel, C., et al., Biodegradable nanoparticles made from polylactide-grafted dextran copolymers .Journal of colloid and interface science, 2009. 330(2): 337-343.
10. Han, D.P., et al., Spectrum and susceptibilities of microbiologic isolates in the Endophthalmitis Vitrectomy Study. American journal of ophthalmology, 1996. 122(1): 1-17.
11. Jelvehgari, M., et al., Formulation, characterization and in vitro evaluation of theophylline-loaded Eudragit RS 100 microspheres prepared by an emulsion-solvent diffusion/evaporation technique. Pharmaceutical Development and Technology, 2010(00): 1-8.
12. Valizadeh, H., et al., A simple and rapid high-performance liquid chromatography method for determining furosemide, hydrochlorothiazide, and phenol red: applicability to intestinal permeability studies. J AOAC Int, 2006. 89(1): 88-93.
13. Zakeri-Milani ,P., et al., Biopharmaceutical classification of drugs using intrinsic dissolution rate (IDR) and rat intestinal permeability. Eur J Pharm Biopharm, 2009. 73(1): p. 102-106.
14. Zakeri-Milani, P., et al., Investigation of the intestinal permeability of ciclosporin using the in situ technique in rats and the relevance of P-glycoprotein. Arzneimittelforschung, 2008. 58(4): 188-192.
15. Zakeri-Milani, P., et al., Predicting human intestinal permeability using single-pass intestinal perfusion in rat. J Pharm Pharm Sci, 2007. 10(3): 368-379.
16. Zakeri-Milani, P., et al., The utility of rat jejunal permeability for biopharmaceutics classification system. Drug Dev Ind Pharm, 2009. 35(12): 1496-1502.
17. Dashevsky, A. and G. Zessin, The effect of ethylcellulose molecular weight on the properties of theophylline microspheres. Journal of microencapsulation, 1997. 14(3): 273-280.
18. Saravanan, M., et al., Ibuprofen-loaded ethylcellulose/polystyrene microspheres: an approach to get prolonged drug release with reduced burst effect and low ethylcellulose content. Journal of microencapsulation, 2003. 20(3): 289-302.
19. Benichou, A., A. Aserin, and N. Garti, Polyols, high pressure, and refractive indices equalization for improved stability of W/O emulsions for food applications. Journal of dispersion science and technology, 2001. 22(2-3): 269-280.
20. Fagerholm, U., M. Johansson, and H. Lennern¤ís, Comparison between permeability coefficients in rat and human jejunum. Pharmaceutical research, (1996) 13(9): 1336-1342.
21. Shantha Kumar, T.R., et al., Validated HPLC analytical method with programmed wavelength UV detection for simultaneous determination of DRF-4367 and Phenol red in rat in situ intestinal perfusion study. Journal of pharmaceutical and biomedical analysis, 2005. 38(1): 173-179.
22. Favetta, P., et al., New sensitive assay of vancomycin in human plasma using high-performance liquid chromatography and

electrochemical detection. Journal of Chromatography B: Biomedical Sciences and Applications, 2001. 751(2): 377-382.
23. Hoffart, V., et al., Low molecular weight heparin-loaded polymeric nanoparticles: formulation, characterization, and release characteristics. Drug Dev Ind Pharm, 2002. 28(9): 1091-1099.
24. Hasan, A.S., et al ,.Effect of the microencapsulation of nanoparticles on the reduction of burst release. Int J Pharm, 2007. 344(1-2): 53-61.
25. Couvreur, P., et al., Nanocapsule technology: a review. Critical reviews in therapeutic drug carrier systems, (2002) 19(2): 99-134.
26. Agnihotri, S.M. and P.R. Vavia, Diclofenac-loaded biopolymeric nanosuspensions for ophthalmic application. Nanomedicine, 2009. 5(1): 90-95.
27. Foster, K.A., M. Yazdanian, and K.L. Audus, Microparticulate uptake mechanisms of in□vitro cell culture models of the respiratory epithelium. Journal of pharmacy and pharmacology, 2001. 53(1): 57-66.
28. Mehnert, W. and K. Mäder, Solid lipid nanoparticles:: Production, characterization and applications. Advanced Drug Delivery Reviews, 2001. 47(2-3): 165-196.
29. Mohanraj, V. and Y. Chen, Nanoparticles-a review. Tropical Journal of Pharmaceutical Research, 2007. 5(1): 561-573.
30. Govender, T., et al., PLGA nanoparticles prepared by nanoprecipitation: drug loading and release studies of a water soluble drug. Journal of Controlled Release, 1999. 57(2): 171-185.
31. Govender, T., et al., Defining the drug incorporation properties of PLA-PEG nanoparticles. International journal of pharmaceutics, 2000. 199(1): 95-110.
32. Panyam, J., et al ,.Solid□state solubility influences encapsulation and release of hydrophobic drugs from PLGA/PLA nanoparticles. Journal of pharmaceutical sciences, 2004. 93(7): 1804-1814.
33. Gavini, E., et al., PLGA microspheres for the ocular delivery of a peptide drug, vancomycin using emulsification/spray-drying as the preparation method: in vitro/in vivo studies. European journal of pharmaceutics and biopharmaceutics, 2004. 57(2): 207-212.
34. Mukherjee, B., et al., A comparison between povidone-ethylcellulose and povidone-eudragit transdermal dexamethasone matrix patches based on in vitro skin permeation. European journal of pharmaceutics and biopharmaceutics, 2005. 59(3): 475-483.
35. Lin, S.Y. and H.L. Yu, Microscopic fourier transform infrared/differential scanning calorimetry system used to study the different thermal behaviors of polymethacrylate copolymers of Eudragits RS, RL, E 30D, or E. Journal of applied polymer science, 2000. 78(4): 829-835.
36. Gribb, A.A. and J.F. Banfield, Particle size effects on transformation kinetics and phase stability in nanocrystalline TiO2. American Mineralogist, 1997. 82(7): 717-728.
37. Kumar, G.S., et al., Synthesis and characterization of bioactive hydroxyapatite-calcite nanocomposite for biomedical applications. J Colloid Interface Sci, 2010. 349(1): 56-62.
38. Fagerholm, U., M. Johansson, and H. Lennernas, Comparison between permeability coefficients in rat and human jejunum. Pharm. Res., 1996. 13: 1336-1342.
39. Amidon, G.L., et al., A theoretical basis for a biopharmaceutic drug classification: the correlation of in vitro drug product dissolution and in vivo bioavailability. Pharmaceutical research, 1995. 12(3): 413-420.
40. Olfert, E.D., et al., Guide to the care and use of experimental animals. Vol. 1. 1993: Canadian Council on Animal Care Ottawa, Ontario, Canada.
41. Danzer, L., Liquid-chromatographic determination of cephalosporins and chloramphenicol in serum. Clinical chemistry, 1983. 29(5): 856-858.
42. Swenson, E.S., W.B. Milisen, and W. Curatolo, Intestinal permeability enhancement: efficacy, acute local toxicity, and reversibility. Pharmaceutical research, 1994. 11(8): 1132-1142.
43. Youan, B.B.C., et al., Protein release profiles and morphology of biodegradable microcapsules containing an oily core. Journal of controlled release, 2001. 76(3): 313-326.
44. Pignatello, R., et al., Properties of tolmetin-loaded Eudragit RL100 and Eudragit RS 100 microparticles prepared by different techniques. STP pharma sciences, 1997. 7(2): 148-157.
45. Malamataris, S. and A. Avgerinos, Controlled release indomethacin microspheres prepared by using an emulsion solvent-diffusion technique. International Journal of Pharmaceutics, 1990. 62(2-3): 105-111.
46. Alex, R. and R. Bodmeier, Encapsulation of water-soluble drugs by a modified solvent evaporation method. I. Effect of process and formulation variables on drug entrapment. Journal of Microencapsulation, 1990. 7(3): 347-355.
47. Xie, J. and C.H. Wang, Self-assembled biodegradable nanoparticles developed by direct dialysis for the delivery of paclitaxel.

Pharmaceutical research, 2005. 22(12): 2079-2090.
48. Ceschel, G., et al., Degradation of components in drug formulations: a comparison between HPLC and DSC methods. Journal of pharmaceutical and biomedical analysis, 2003. 32(4-5): 1067-1072.
49. Jelvehgari, M., et al., Control of encapsulation efficiency in polymeric microparticle system of tolmetin. Pharmaceutical development and technology, 2010. 15(1): 71-79.
50. Aaltonen ,J., et al., Polymorph screening using near-infrared spectroscopy. Analytical Chemistry, 2003. 75(19): 5267-5273.
51. Gupta, M. and T. Saini, preformulation parameters characterization to design, development and formulation of vancomycin hydrochloride tablets for psudomembranous colitis. international Journal of pharmaceutical reaserch and development, 2009. 1(9).
52. Jelvehgari, M., et al., Preparation and Evaluation of Poly (-caprolactone) Nanoparticles-in-Microparticles by W/O/W Emulsion Method. Iranian Journal of Basic Medical Sciences, 2010. 13(3): 1-8.
53. Capan, Y., et al., Preparation and characterization of poly(D,L-lactide-co-glycolide) microspheres for controlled release of human growth hormone. AAPS PharmSciTech, 2003. 4(2): E28.
54. Yang, Y.-Y., T.-S. Chung, and N. Ping Ng, Morphology, drug distribution, and in vitro release profiles of biodegradable polymeric microspheres containing protein fabricated by double-emulsion solvent extraction/evaporation method. Biomaterials, 2001. 22(3): 231-241.
55. Wu, J.C., et al., Effect of the solvent-non-solvent pairs on the surface morphology and release behaviour of ethylcellulose microcapsules prepared by non-solvent-addition phase separation method. J Microencapsul, 1994. 11(3): 297-308.
56. Wickramasinghe, R., J.L. Liow, and Y.K. Leong. Nanobiotech congress. 2007; Available from: http://www.aiche.org/uploadedfiles/SBE/events/Tuesday07.pdf.
57. Martin, A., P. Bustamante, and A.H. Chun, Physical Pharmacy and Pharmaceutical Sciences. Fifth edition ed2006, Philadelphia: Lippincott Williams & Wilkins.
58. Mondal, S., et al. Flocculation of yeast suspension by a cationic polymer: Characterization of flocculent-cell interaction. 2011. American Institute of Chemical Engineers.
59. Mukherjee ,B., et al., Preparation, characterization and in-vitro evaluation of sustained release protein-loaded nanoparticles based on biodegradable polymers. Int J Nanomedicine, 2008. 3(4): 487-496.
60. Fonseca, C., S. Simoes, and R. Gaspar, Paclitaxel-loaded PLGA nanoparticles: preparation, physicochemical characterization and in vitro anti-tumoral activity. J Control Release, 2002. 83(2): 273-286.
61. Ahlin, P., et al., Investigation of polymeric nanoparticles as carriers of enalaprilat for oral administration. Int J Pharm, 2002. 239(1-2): 113-120.

